

# Parameter sensitivity of a watershed-scale flood forecasting model as a function of modelling time-step

Fiachra O'Loughlin, Michael Bruen and Thorsten Wagener

## ABSTRACT

Although ongoing technological advances have alleviated data restrictions and most of the computational barriers to distributed modelling, lumped, parsimonious, conceptual and rainfall-runoff models are still widely used for flood forecasting. However both optimum parameter values and the fluxes of water through individual model components change significantly with the time-step used. Thus, such models should be used with caution in applications such as hydrograph separation or water quality studies that require the fluxes through individual flow routes through the model or which try to relate parameters to physical features of the catchment. To demonstrate this time-scale limitation, a parameter sensitivity analysis was performed on the lumped conceptual Soil Moisture Accounting and Routing with Groundwater component (SMARG) model for a 182 km<sup>2</sup> rural catchment in Ireland for a number of time-steps, flow regimes and evaluation metrics. A global sensitivity analysis method (Higher Dimensional Model Representation) showed that sensitivity indices vary greatly with time-step and evaluation metric. The sensitivity of parameters also varied for different flow regimes. Certain parameters' sensitivities remain fairly constant across both flow regimes and time-step, while others are very much regime or time-step dependent. Care should be taken in using internal information from conceptual models because of this strong dependence on time-step.

**Key words** | flood forecasting, rainfall-runoff modelling, sensitivity analysis, SMARG, time-step

### Fiachra O'Loughlin

School of Geographical Sciences,  
University of Bristol,  
University Road,  
Bristol BS8 1SS,  
UK

### Michael Bruen (corresponding author)

School of Civil, Structural and Environmental  
Engineering,  
University College Dublin 4,  
Ireland  
E-mail: michael.bruen@ucd.ie

### Thorsten Wagener

Department of Civil Engineering,  
University of Bristol,  
Queen's Building, University Walk,  
Bristol BS8 1TR,  
UK

## INTRODUCTION

In the last decade, flooding has affected millions of people in many parts of the world, with large scale flooding events in Central Europe in 2002, Eastern and Central Europe in 2005, the South of England in 2007, Ireland in both 2008 and 2009 and Australia in 2011. Flooding is likely to become more frequent and severe due to the anticipated effects of climate change (Bates *et al.* 2008). Min *et al.* (2011) suggest that some climate models may underestimate extreme precipitation events and that these events may intensify quicker and have more severe impacts than projected. Pall *et al.* (2011) looked at the contribution of anthropogenic greenhouse gases to flood risk and concluded that these gases 'substantially increased' the flooding risk in England and Wales. The climate of Ireland is expected to change dramatically by 2050 with wetter winters and drier

summers. In the winter months, rainfall events are predicted to be longer in duration and in the summer, less frequent but more intense events will occur (Dunne *et al.* 2008). Both situations will lead to an increase in flood risk in both winter and summer and flood forecasting will become even more important as part of an integrated flood risk management strategy.

Rainfall-runoff models are key elements for flood forecasting and understanding their functional behaviour and limitations is essential to engender trust in the model and confidence in its output. Lumped rainfall-runoff models have, in some cases, shown advantages over spatially distributed models for flood forecasting. For instance, Refsgaard & Knudsen (1996) recommended the use of a lumped conceptual model over semi- and fully distributed models in runoff

forecasting, due to the effort involved in the setup of more complex models. Bell & Moore (1998) found that a lumped model was as good as a distributed model in most flood forecasting cases and suggested that a well calibrated lumped rainfall-runoff model is to be preferred for operational flood forecasting, although there are some cases in which semi-distributed models outperformed their lumped counterparts (see among others Moreda *et al.* (2006); Pechlivanidis *et al.* (2010)).

Sensitivity analysis evaluates the impact of change in the model parameters, inputs or (initial) states on the model output. For instance, sensitivity analysis has been used to explore models' high-dimensional parameter space, evaluate the impact of rainfall error, and improve parameter identifiability (see among others Hossain *et al.* (2004); Sieber & Uhlenbrook (2005); Demaria *et al.* (2007); Tang *et al.* (2007a, 2007b); Fenicia *et al.* (2008); McIntyre & Al-Qurashi (2009); van Werkhoven *et al.* (2009); Wagener *et al.* (2009); Younger *et al.* (2009)).

Across a wide range of disciplines, there are many different methods used to determine the sensitivity of models to their parameters. Variance based methods (Sobol 1993; Saltelli 2002) and the Regional Sensitivity Analysis (RSA) (Bastidas *et al.* 1999; Spear & Hornberger 1981) have been widely used in hydrology. Tang *et al.* (2007b) compared different sensitivity analysis methods and found that a variance-based method (Sobol 2001) gave the most robust results, even though it required considerable computational effort. Wagener *et al.* (2009) noted that the choice of model performance measure had a significant influence on the sensitivity of the parameters.

The influence of modelling time-step is significant in flood forecasting and in rainfall-runoff modelling in general. Littlewood (2007) and Littlewood & Croke (2008) noted that, as the time-step decreased, initially, the parameter values for a simple rainfall-runoff model could change by between 52 and 81%, but generally a time-step is reached, below which the parameters values stabilised without any further change with decrease in time-step. Clarke & Kavetski (2010) noted that it is difficult to pre-determine a fixed time-step that always gives the best results. They and others, for example, Kavetski & Clarke (2010) and Schoups *et al.* (2010), suggest using time-stepping schemes, which can give better accuracy but with higher computational costs.

This paper has three main objectives, all relating to the parameter sensitivity of flood forecasting models. The first is to test the Higher Dimensional Model Representation (HDMR) method (Ziehn & Tomlin 2008a) for calculating parameter sensitivity indices, which are the ratios of the marginal change in some function of the model output to the change in parameter value causing it. The second objective is to add to the work of van Werkhoven *et al.* (2008), who evaluated model performance at daily and hourly time-steps, by using still smaller time-steps often required in flood forecasting, e.g. 15 minutes, for a number of different evaluation metrics. The third objective is to show which parameters of the SMARG (Soil Moisture Accounting and Routing with Groundwater component) rainfall-runoff model (Tan & O'Connor 1996) are important for simulating flood flows. Finally, this paper investigates some issues that arise when using dimensionally consistent temporal scaling of parameters in conceptual modelling, i.e. scaling each parameter in the model according to the time component of its dimension. The paper has five main sections: the introduction; a description of the test catchment and data; a description of the model used, the method of sensitivity analysis, the evaluation metrics and the approach; results and discussion, and finally the summary and conclusions.

## DATA

The Nanny Catchment lies to the North of Dublin City on the East coast of Ireland (Figure 1). The Nanny River rises at Carn Hill, which is located immediately East of Navan and drains into the Irish Sea with a catchment area of 218 km<sup>2</sup>. However, the gauging station furthest downstream (0811) is located near Duleek and its catchment area is 182 km<sup>2</sup> with a channel length of 21 km. Its landscape is rural and gently sloping (its elevation varies between 16 and 162 m above sea level). The Nanny has one major tributary, the Hurley, which joins it approximately 4 km upstream of Duleek. While the Hurley is the longer, with a length of 26 km to the confluence, the Nanny is the larger in terms of flow.

The Precipitation Accumulation Model (PAC) was used to provide estimates of precipitation. PAC is a standard product of the radar station located around Dublin Airport provided by the Irish Meteorological Service, Met Eireann.

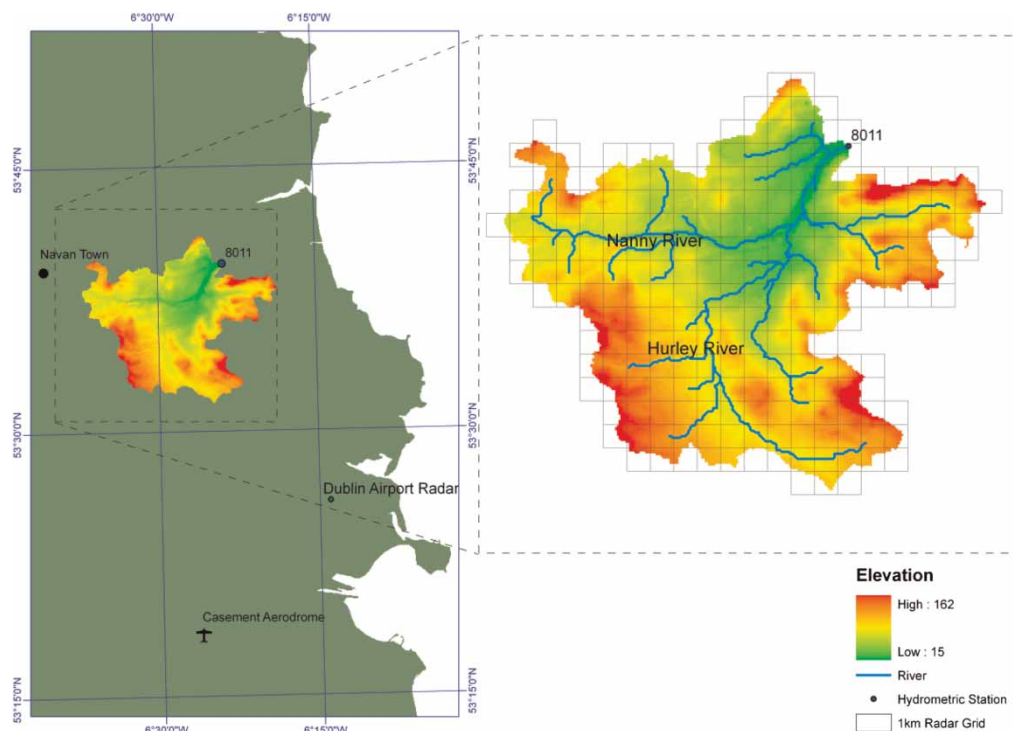


**Figure 1** | The Nanny Catchment, Ireland.

Precipitation is estimated for 15-minute intervals and contains rainfall intensities ( $\text{mm h}^{-1}$ ) on a 1 km grid for an elevation 1 km above the topographical elevation. The range of the PAC model is approximately 70 km and includes the entire Nanny catchment. The PAC gives rainfall intensities at 15-minute intervals from which the hourly and daily precipitation estimates were obtained. An appropriate gauge adjustment factor, 1.45, was obtained by comparing the daily precipitation estimates from the radar and 20 rain gauges located at a variety of distances from the radar.

A daily potential evaporation (PE) dataset was also obtained from Met Eireann for Casement Aerodrome (see Figure 1). Daily PE records were disaggregated to hourly data using the WDMUtil program (USEPA 2010) based on latitude and time of the year, with most evaporation occurring during daylight hours. Hourly evaporation data were disaggregated into 15-minute records assuming a uniform distribution; hence  $PE_{15} = PE_{\text{hourly}}/4$ .

Flow data (both discharge and water levels) for the Nanny River at Duleek (station 0811) were obtained at

15-minute intervals from the Office of Public Works, OPW. Due to the small time-steps and large amount of data involved, this study concentrates on a single year (2002), which experienced significant floods. This year was selected from a 9-year period (2001–2009), as there were less periods of missing data during that year yet contained the greatest variety in flow regimes. Missing data (6.5% of the total period) were excluded from the analysis.

## METHOD

### SMARG model

The SMARG model (Khan 1986; Liang 1992; Uhlenbrook *et al.* 1999) is a modified version of the Soil Moisture Accounting and Routing (SMAR) model. The SMARG is a lumped, conceptual, rainfall-runoff model, initially developed as the *layers model* (O'Connell *et al.* 1970; Saltelli 2000), in which the soil water-balance is based on the 'Layers Water Balance Model' of Nash & Sutcliffe (1970).

The SMARG model (Figure 2) consists of two distinct components. The first is a non-linear soil moisture accounting component that keeps account of the water balance between rainfall, evaporation, runoff, and soil storage using a number of empirical functions, which are assumed to be physically plausible. The second is the routing component, which simulates the attenuation and the diffusive effects of the catchment by routing the different components of runoff generated by the water balance calculations through linear time-invariant storage systems.

The catchment is represented as a set of horizontal soil layers (the number of layers varies between 1 and 5), each of which may contain water up to a maximum depth of 25 mm except for the bottom layer, which may have a larger depth. The maximum soil moisture storage capacity ( $Z$ ; sum of water depths of all layers) varies between 25 and 125 mm

(see Table 1). A multiplier  $T$  is used to convert the PE to potential evapotranspiration (PET) for the entire catchment. The PET demand is firstly subtracted from rainfall input and water evaporates from the soil layers only when this is insufficient to satisfy the PET demand or when there is no rainfall. Evaporation from the first layer occurs at the PET rate. Evaporation from the lower layers occurs only after the layer above has dried out and occurs at a rate of PET multiplied by  $C^{n-1}$ , where  $n$  is the layer index and  $C$  is the evaporation decay coefficient ( $<1$ ). Evaporation continues until either the PET demand is satisfied or no soil moisture is left to evaporate.

When rainfall ( $R$ ) exceeds PET, direct or saturation excess runoff is generated. A fraction  $H'$  of the excess rainfall  $X$  (equals  $R - PET$ ) contributes to the direct runoff component  $r_1$ .  $H'$  varies in time between 0 and 1 and is assumed equal to the direct runoff separation coefficient

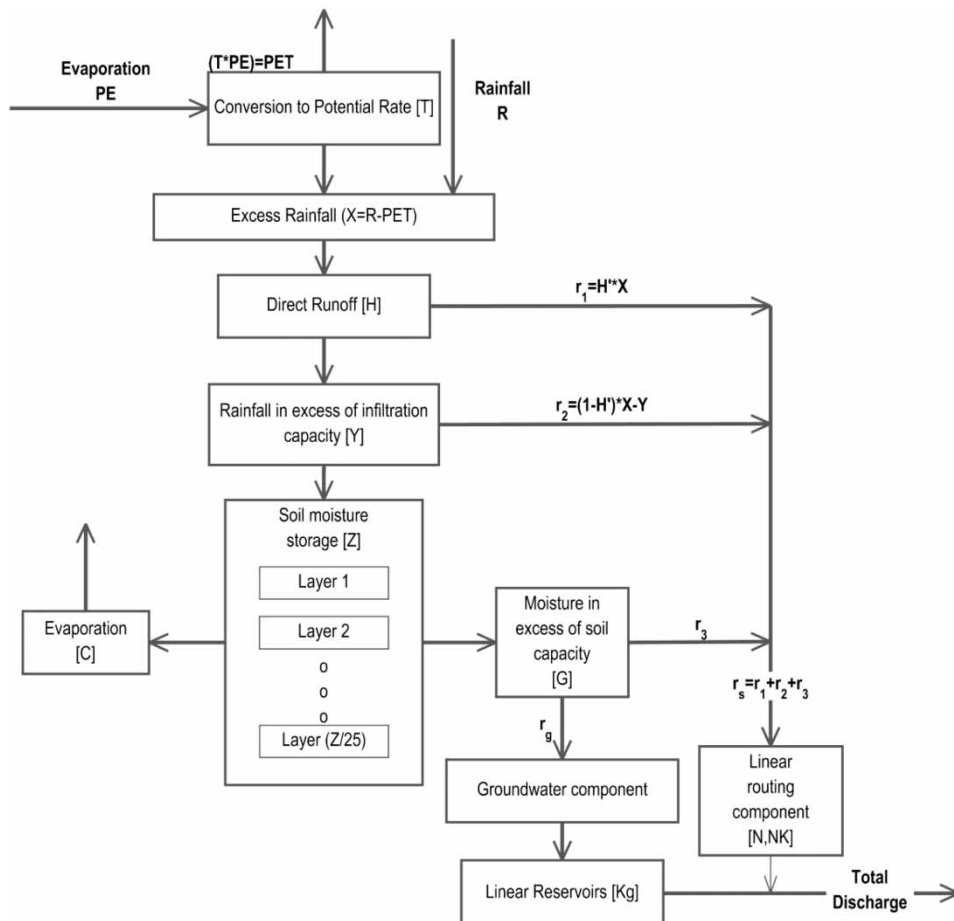


Figure 2 | Schematic representation of the SMARG model structure (reproduced from Liang (1992)).

**Table 1** | Parameters of the SMARG model and their daily ranges

Parameter	Description	Lower Limit	Upper Limit
T	Potential evaporation conversion coefficient (-)	0.5	1
H	Direct runoff separation coefficient (-)	0	1
Y	Maximum soil moisture infiltration rate (mm/day)	10	100
Z	Soil moisture capacity (mm)	25	125
C	Evaporation decay coefficient (day <sup>-1</sup> )	0.5	1
G	Groundwater separation coefficient (-)	0	1
N	Number of linear reservoirs in cascade (-)	1	10
NK	Time-lag parameter for Nash cascade routing (day)	1	10
Kg	Time-lag parameter for groundwater storage (day)	1	200

( $H$ ) multiplied by the relative saturation of the catchment according to ( $W$  is the soil moisture storage):

$$H' = H \frac{W}{Z} \quad (1)$$

Any remaining excess rainfall which exceeds the maximum infiltration capacity ( $Y$ ), also contributes, as Hortonian runoff, to the generated runoff as  $r_2$ . The remaining rainfall after the subtraction of  $r_1$  and  $r_2$  replenishes the soil layers in turn beginning with the upper layer and moving downwards until all the rainfall is accounted for or all the layers are full. Any still remaining surplus is divided into two fractions controlled by a separation coefficient  $G$ ; the first being the groundwater runoff component  $r_g$ , and the second being the subsurface runoff  $r_3$ .  $r_3$  is added to  $r_1$  and  $r_2$  to produce the total generated surface runoff  $r_s$ . The total generated surface runoff is routed through one of a number of possible two-parameter distribution functions, either the gamma distribution with shape parameter ( $N$ ) and lag parameter ( $NK$ ), or the Negative Binomial distribution or the Inverse Gaussian distribution (in this study, we use the gamma distribution). The groundwater runoff component,  $r_g$ , is routed through a single linear reservoir with a storage coefficient parameter ( $Kg$ ). The sum of the two outputs of the two routing components is the estimated streamflow.

The SMARG model has nine parameters (see Table 1), five of which control the overall water-budget component, while the remaining four parameters control the routing operations. SMARG requires data series of precipitation and potential evaporation for simulation and a corresponding flow time-series for calibration. The model can run at any time-step, but hourly or daily time-steps are typical.

### HDMR

The HDMR method is a set of tools to express in a generalised way the input-output relationship of complex models with large numbers of input parameters (Rabitz et al. 1999). It expresses this relationship as the sum of a series of terms of increasing order and increasing number of interactions between parameters, as shown in Equation (2):

$$f(x) = f_0 + \sum_{i=1}^n f_i(x_i) + \sum_{1 \leq i < j < n} f_{ij}(x_i, x_j) + \dots + f_{1,2,n}(x_1, x_2, \dots, x_n) \quad (2)$$

where  $f_0$  is a constant,  $f_i(x_i)$  is a first order term giving the effect of parameter  $x_i$  acting independently,  $f_{ij}(x_i, x_j)$  are second order terms describing the interactive effect of parameters  $x_i$  and  $x_j$  on the output  $f(x)$ . The higher order terms reflect the cooperative effects of increasing numbers of parameters acting together.

The HDMR expansion is computationally efficient if higher order interactions are weak (Ziehn & Tomlin 2008a). Other hydrological studies have used an expansion up to second order and have achieved satisfactory results (see among others Tang et al. (2007b)).

HDMR is implemented in the graphical user interface (GUI)-HDMR Matlab toolbox and is based on the existing regularized random-sampling high dimensional model representation (RS-HDMR) tools and extensions (Ziehn & Tomlin 2008a). This toolbox approximates the component functions using orthonormal polynomials. The zero order term  $f_0$  can be approximated by the average value of  $f(x)$ . The determination of the higher order component functions are based on the approximation of the component functions



by orthonormal basis functions:

$$f_i(x_i) \approx \sum_{r=1}^k \alpha_r^i \varphi_r(x_i) \quad (3)$$

$$f_{ij}(x_i, x_j) \approx \sum_{p=1}^l \sum_{q=1}^r \beta_{pq}^{ij} \varphi_p(x_i) \varphi_q(x_j) \quad (4)$$

where  $k, l, r$  represent the order of the polynomial expansion,  $\alpha_r^i$  and  $\beta_{pq}^{ij}$  are constant coefficients to be determined and  $\varphi_r(x_i), \varphi_p(x_i), \varphi_q(x_j)$  are the orthonormal basis functions. An optimisation method automatically chooses the best polynomial order for the approximation of each of the component functions and a threshold automatically excludes unimportant component functions (Ziehn & Tomlin 2008a, 2008b).

Parameter sensitivity is based on the contribution to the total variance ( $D$ ) from the first and second order variances,  $D_i$  and  $D_{ij}$ , respectively (Li *et al.* 2002; van Werkhoven *et al.* 2009). The total variance is given by Equation (5), which can be further approximated by Equation (6):

$$D = \int [f(x) - f_0]^2 dx \quad (5)$$

$$D = \int_{k^n} f^2 dx - f_0^2 \quad (6)$$

The first and second order variances are given by Equations (7) and (8), respectively:

$$D_i = \int_0^1 f_i^2(x_i) dx_i \quad (7)$$

$$D_{ij} = \int_0^1 \int_0^1 f_{ij}^2(x_i, x_j) dx_i dx_j \quad (8)$$

Once the partial variances are determined, sensitivity indices are calculated as follows:

$$S_i = \frac{D_i}{D} \quad (9)$$

$$S_{ij} = \frac{D_{ij}}{D} \quad (10)$$

The first order sensitivity index  $S_i$  measures the effect of variable  $x_i$  on  $f(x)$ . The second order sensitivity index  $S_{ij}$  measures the strength of the interaction effects of  $x_i$  and  $x_j$  on  $f(x)$ .

To our knowledge, HDMR has drawn little attention in hydrology, however the method has been applied in other fields e.g. chemistry (Skodje *et al.* 2010; Davis *et al.* 2011), medicine (Blanchard *et al.* 2011) and environmental modelling (Ziehn *et al.* 2009). HDMR is conceptually similar to the Sobol method (Sobol 1993, 2001) which has been recently used in hydrology (van Werkhoven *et al.* 2009; Wagener *et al.* 2009; Cibin *et al.* 2010).

### Metrics for model evaluation

Two different and widely used, metrics for model output evaluation were used to assess the sensitivities of the SMARG model parameters. The Nash Sutcliffe efficiency (NSE) (Nash & Sutcliffe 1970) has been widely applied in hydrological modelling and is defined as:

$$NSE = 1 - \frac{\sum_{t=1}^n (Q_{o,t} - Q_{m,t})^2}{\sum_{t=1}^n (Q_{o,t} - \bar{Q}_0)^2} \quad (11)$$

where  $Q_{o,t}$  is the observed flow for time-step,  $t$ ,  $Q_{m,t}$  is the modelled flow at time-step  $t$ , and  $n$  is the length of the time series. The second metric used is the mean bias (BIAS) defined as:

$$BIAS = \frac{1}{n} \sum_{t=1}^n (Q_{o,t} - Q_{m,t}) \quad (12)$$

These two metrics were chosen as they focus on different aspects of the comparison. NSE focuses on the correlation between the time-series, while BIAS focuses on the overall water balance.

### Approach

Sensitivity analysis of the SMARG hydrological model was conducted for daily, hourly and 15-minute model time-steps. For each of the model time-steps, 50,000 Monte Carlo parameter sets in which randomly sampled and their

corresponding outputs were compared to the observed flow using the two evaluation metrics (NSE and BIAS). The comparison was done for three different time-periods: (1) the entire period (year 2002) neglecting the first 30 days to reduce to the influence of choice of the initial catchment conditions; (2) a predominantly high flow period within that year; and (3) a predominantly low flow period within that year. Figure 3 presents the observed flow at Station No. 8011 and the catchment average precipitation for the year 2002 (and also the three time periods analysed). Parameter sensitivity was calculated using the HDMR model; this model analyses the 50,000 parameter samples and their corresponding evaluation metrics, resulting in 18 sets of parameter sensitivities. A 'set' refers to a group of nine parameter sensitivity indices for first and second order indices for each individual analysis period and for each evaluation metric. Thus the results cover all combinations (scenarios) of:

- (i) the three model time-steps (15 min, hourly, daily)
- (ii) the two evaluation metrics (NSE and BIAS)
- (iii) the three periods of flow regime (low flow, high flow and entire period).

To show the effects of dimensionally consistent scaling, the model was evaluated at daily, hourly and 15-minute time-steps. Optimised parameter values were obtained using a global optimisation method for each of the time-steps. The optimised parameters for each time-step were further scaled in a dimensionally consistent way to produce scaled parameters for the other two time-steps. This resulted in three parameter sets for each model time-step. The proportion of each component to the total rainfall and flow is determined for every parameter set; the components are presented in Table 2.

## RESULTS AND DISCUSSION

Figure 4 illustrates the parameter sensitivity indices (first, second and combined sensitivities) for each evaluation metric simulation time-step and flow regime. Highly sensitive parameters have a sensitivity index greater than 0.1 (van Werkhoven *et al.* 2008). Table 3 lists the highly sensitive parameters, whose combined first and second order

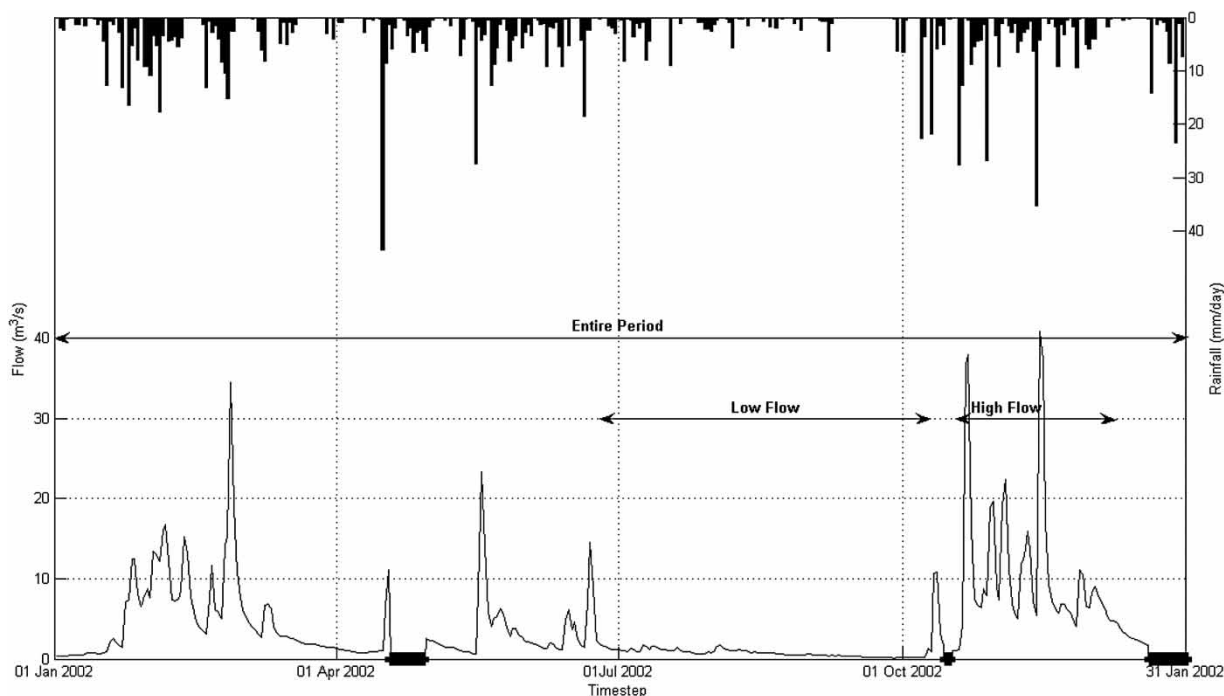


**Figure 3** | Catchment precipitation time series and discharge at Station No. 8011 for the year 2002. Different evaluation periods are shown (thicker line indicates periods of missing discharge data).

**Table 2** | Output fluxes and components

Output Flux	Component	Variable
Runoff	Saturation excess runoff	$r_1$
	Hortonian runoff	$r_2$
	Subsurface runoff	$r_3$
	Groudwater discharge	$r_g$
Surface Evaporation	-	-
Soil Evapotranspiration	-	-

sensitivities are greater than 0.1, with respect to evaluation method, analysis period and model time-step.

The best Monte Carlo run for a daily time-step is shown in Figure 5. This model achieved an NSE equal to 0.72 and a BIAS equal to 0.16 mm day<sup>-1</sup>. The best results achieved for each of the evaluation metrics and for each analysis period are shown in Table 4, which shows that the SMARG model

with the best of the Monte Carlo parameter sets can model the observed hydrograph with some accuracy. However, it should be noted that these are not optimised parameters.

**Performance measures**

**Performance measure 1: Nash Sutcliffe efficiency**

The sensitivity analysis of the daily runs of the SMARG model shows that the groundwater separation coefficient (G) is important across all the analysis periods. G controls the ratio of moisture in excess of the soil moisture capacity that goes to either subsurface runoff or groundwater runoff. Thus during the low flow period, the model favours a high value of G so that most excess water passes through the groundwater component. For high flow periods, the value of G may be lower so

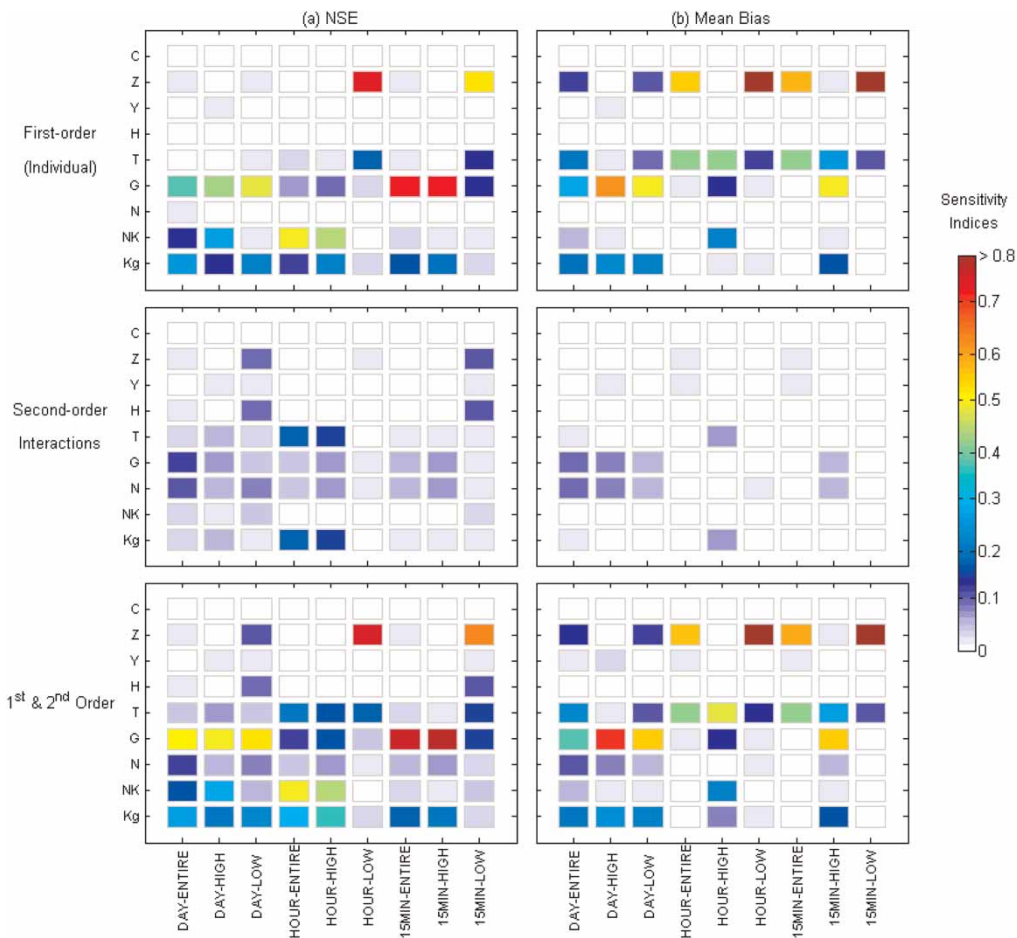


**Figure 4** | Sensitivity indices for nine parameters and each modelling scenario: first order (individual contributions), second order (interaction contributions), and first and second order for (a) NSE, and (b) mean bias.



**Table 3** | Summary of sensitive parameters showing influence on time-step and performance measure

Model Interval	Analysis Period					
	NSE			Mean Bias		
	Entire	High Flow	Low Flow	Entire	High Flow	Low Flow
Day	G, Kg, NK,N	G, NK, Kg	G, Kg, Z, H	G, T, Kg, Z, N	G, Kg, N	G, Kg, Z, T
Hour	N K, Kg, T, G	NK, Kg, T, G	Z, T	Z, T	T, N K, G, Kg	Z, T
15 minute	G, Kg	G, Kg	Z, H, G, T	Z, T	G, T, Kg	Z, T

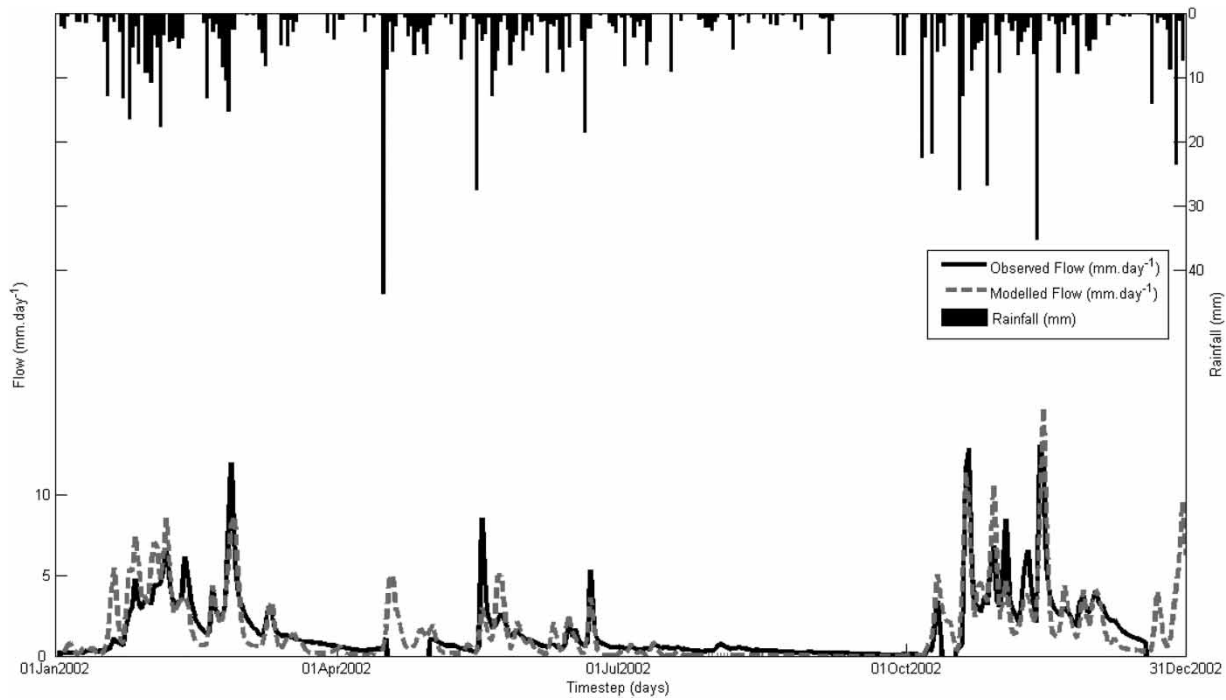


**Figure 5** | Modelled flow using the best Monte Carlo run for daily time-step (NSE = 0.72 and BIAS = 0.16 mm/day).

**Table 4** | Best model performance for each time-step and performance measure using Monte Carlo parameter sets

Model Interval	Analysis Period					
	NSE			BIAS (mm/day)		
	Entire	High Flow	Low Flow	Entire	High Flow	Low Flow
Daily	0.72	0.69	0.87	0.08	0.13	0.08
Hourly	0.74	0.65	0.90	0.24	0.07	0.22
15 minute	0.73	0.67	0.90	0.28	0.14	0.25

that the correct proportion of the excess water is routed through both subsurface and groundwater runoff.

As expected, using a daily time-step, the time-lag of the Nash cascade routing (NK) was important for the high flow period but not for the low flow period, as NK along with N controls the shape of the flood hydrograph. The time-lag for the groundwater storage (Kg) was important during both high and low flow periods. Kg controls the recession curve of the groundwater flow and in this catchment groundwater contribution is significant during both wet and dry periods. It is interesting to note the importance of the direct runoff coefficient ( $H$ ) during the low flow period, as it was expected to be significant only at the high flows.  $H$  controls the division of excess rainfall between surface runoff and/or subsurface flow. During low flow periods, most of the total discharge comes from subsurface flow, so a high  $H$  value would result in mostly surface runoff.

In contrast, for the hourly runs, the potential evaporation conversion coefficient ( $T$ ) was important across all the analysis periods. In particular, during the low flow period when no significant rainfall events occur, evaporation loss increases, hence the water balance is expected to be influenced by  $T$ . In addition, the sensitivity to  $T$  for high flow periods is explained by the need to generate sufficient effective rainfall to reproduce the peak discharges. Figure 6 illustrates the effect of  $T$  on model output. Increasing the value of  $T$  from

0.799 to 0.999 (hence 40% greater evaporation losses) reduces the total volume of runoff by 30%.

Using hourly and 15-minute time-steps, a number of parameters were important for the entire analysis period and the high flow period. The time-lag of the Nash cascade routing (NK), the time-lag for the groundwater storage (Kg) and the groundwater separation coefficient ( $G$ ) were important for the same reasons mentioned earlier for daily runs. For the low flow period and for hourly time-steps, the soil moisture storage capacity ( $Z$ ) was important for the same reasons mentioned earlier. However, when a 15-minute time-step was used the potential evaporation conversion coefficient ( $T$ ), the direct runoff coefficient ( $H$ ) and the soil moisture storage capacity ( $Z$ ) became more important.

#### Performance measure 2: mean bias

Analyzing the results using daily time-steps with respect to the mean bias for all the analysis periods, the groundwater separation coefficient ( $G$ ) and the time-lag for the groundwater storage (Kg) were found to be important. This is the same as for the Nash–Sutcliffe criterion and for the same reasons. For the low flow period, the soil moisture storage capacity ( $Z$ ), and the potential evaporation multiplier ( $T$ ) were also identified as important. The sensitivity of  $Z$  for the entire

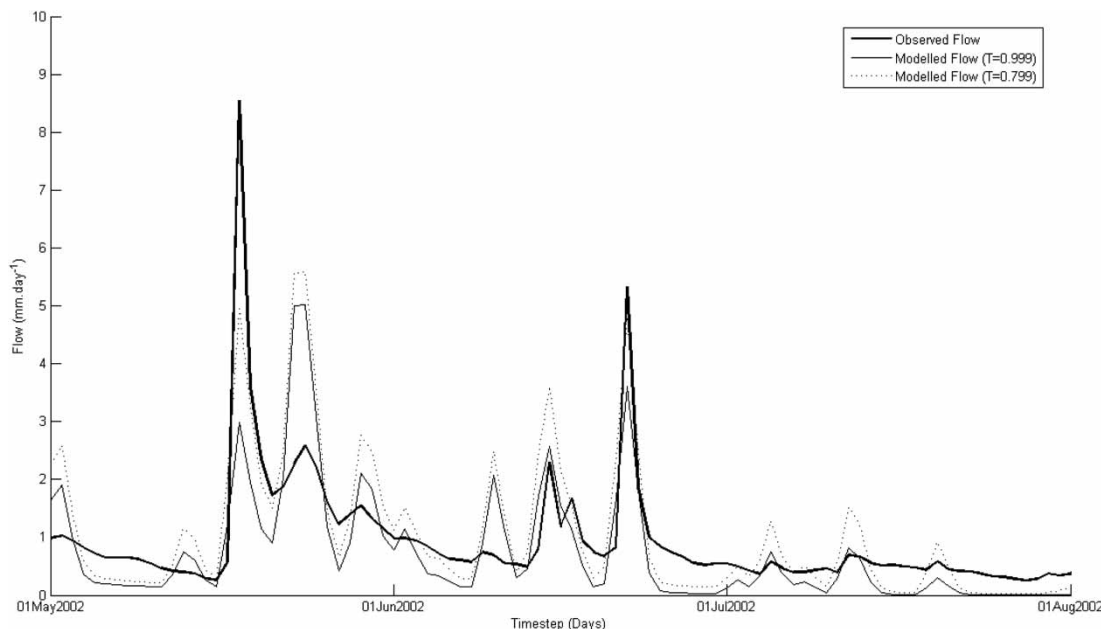


Figure 6 | Effect of PET conversion coefficient ( $T$ ) on modelled discharge (daily time-step).

period is due to the temporal variability of the rainfall. In the analysis that uses data for the entire year, there are periods of: (1) low or no rainfall (daily rainfall is less than  $0.1 \text{ mm day}^{-1}$ ) and hence only small amounts of moisture in the soil, and (2) periods of high rainfall (daily rainfall is greater than  $15 \text{ mm day}^{-1}$ ), in which the soil moisture capacity is reached or exceeded. A high value of  $Z$  during the low flow period would result in little or no subsurface or groundwater runoff, so that the model can produce some runoff to match the observed hydrograph. The sensitivity of parameters  $N$  and  $NK$  for the entire and high flow periods was expected as both parameters control the shape of the hydrographs.

The potential evaporation conversion coefficient ( $T$ ) seems to be important for the same reasons as for the NSE for all the analysis periods using hourly time-steps. For the entire analysis period and the low flow period, the soil moisture storage capacity ( $Z$ ), was also identified as important. There are periods of little rainfall in which the associated discharge is mostly due to subsurface and groundwater runoff, and therefore must allow adequate subsurface and groundwater flow generation to match the observed hydrograph. For the high flow period, the groundwater separation coefficient ( $G$ ), the time-lag of the Nash cascade routing ( $NK$ ) and the time-lag for the groundwater storage ( $Kg$ ) were also identified as important.

Some common traits were identified using the 15-minute runs. These traits were almost identical to those found for the hourly runs with the exception of the time-lag of the Nash cascade routing ( $NK$ ), which was not deemed sensitive for the 15-minute time-step runs.

### Dimensionally consistent scaling of parameters

This section highlights the artefacts that can arise with the scaling of parameters between different time-steps. Three sets of optimised parameters are used, one for each time-step. These optimised parameters were then scaled according to their dimension to the other time-steps. Table 5 shows the parameter values used for each time-step. If time is a dimension of the parameter, the parameter value was scaled on the basis of the time-step to ensure comparability. Out of the nine SMARG parameters, only four ( $Y$ ,  $C$ ,  $NK$  and  $Kg$ ) required scaling as the others do not have a time dimension.

Table 6 shows the percentage of total rainfall accounted for by the six components of the SMARG model (saturation

excess runoff ( $r_1$ ), Hortonian runoff ( $r_2$ ), subsurface runoff ( $r_3$ ), groundwater runoff ( $r_g$ ), soil evaporation and potential evaporation), and Table 7 shows the percentage of total streamflow accounted by the four runoff routes ( $r_1$ ,  $r_2$ ,  $r_3$  and  $r_g$ ). These tables highlight the danger of linearly scaling the parameters of a nonlinear conceptual model even if conducted in a dimensionally consistent way. For the daily time-step, while the percentages of flow in the 'surface runoff' (the summation of  $r_1$ ,  $r_2$  and  $r_3$ ), and the groundwater runoff are fairly consistent with each other, the proportion of each pathway of the 'surface runoff' vary considerably between the time-steps. Thus, when parameters optimised for a daily time-step are used  $r_1$ ,  $r_2$ , and  $r_3$  accounted for 19.6, 0, and 28.8%, respectively, of the total streamflow. This changes to  $r_1 = 14.8$ ,  $r_2 = 0.0$  and  $r_3 = 29.6\%$ , when the scaled hourly optimised values were used at a daily time-step, while when the scaled 15-minute optimised parameters were used,  $r_1 = 4.3$ ,  $r_2 = 0.0$  and  $r_3 = 39.6\%$ . While the percentage of direct/saturation excess runoff remains constant with respect to the parameter set used, it is interesting to note the significant difference between the daily and the hourly run and/or the 15-minute run for the partitioning between Hortonian runoff, the subsurface runoff, and the groundwater runoff. These differences could be due to the nonlinear way in which the model determines the amount of water infiltrated into the soil, controlled by parameter  $Y$ . This is supported by Figure 7 which shows that for the hourly and 15-minute runs there are periods during which the excess rainfall exceeds the maximum soil infiltration rate ( $Y$ ) and as a result Hortonian runoff is produced. The proportion of evapotranspiration remains fairly consistent across all the three time-steps. However, the amount of water output through each of the model components, shown in Table 2, varies greatly between the daily time-step and the hourly and/or 15-minute time-steps. For the daily time-step, the losses due to soil evapotranspiration are at least 20% of the total rainfall and losses due to PET are approximately equal to 20% of the rainfall. These losses change to 29% and 8% for the soil evaporation and PET, respectively, for the hourly time-step. The percentages for the 15-minute time-steps are roughly equal to those for the hourly time-step. The changes in the percentage of losses due to PET can be explained by the very low PET rates during night-time; rainfall falling during the night

**Table 5** | Parameter values used for dimensional consistency

<b>Daily time-step</b>				
<b>Parameters</b>	<b>Unit</b>	<b>Daily Opt</b>	<b>Scaled Hourly Opt</b>	<b>Scaled 15-min Opt</b>
T	–	0.81	0.86	0.94
H	–	0.18	0.04	0.13
Y	mm/day	49.06	114.38	100.01
Z	mm	37.44	35.65	33.96
C	/day	0.50	15.00	85.41
G	–	0.64	0.59	0.65
N	–	10.00	2.63	2.54
NK	day	2.09	1.02	1.06
Kg	day	18.21	15.04	15.16
<b>Hourly time-step</b>				
<b>Parameters</b>	<b>Unit</b>	<b>Scaled Daily Opt</b>	<b>Hourly Opt</b>	<b>Scaled 15-min Opt</b>
T	–	0.81	0.86	0.94
H	–	0.18	0.04	0.13
Y	mm/hour	2.04	4.77	4.17
Z	mm	37.44	35.65	33.96
C	/hour	0.02	0.63	3.56
G	–	0.64	0.59	0.65
N	–	10.00	2.63	2.54
NK	hour	50.15	24.56	25.55
Kg	hour	437.11	360.85	363.73
<b>15-minute time-step</b>				
<b>Parameters</b>	<b>Unit</b>	<b>Scaled Daily Opt</b>	<b>Scaled Hourly Opt</b>	<b>15-min Opt</b>
T	–	0.81	0.86	0.94
H	–	0.18	0.04	0.13
Y	mm/15 min	0.51	1.19	1.04
Z	mm	37.44	35.65	33.96
C	/15 min	0.01	0.16	0.89
G	–	0.64	0.59	0.65
N	–	10.00	2.63	2.54
NK	15 min	200.61	98.24	102.20
Kg	15 min	1748.46	1443.39	1454.91

does not evaporate immediately and either infiltrates into the soil or becomes direct/saturation excess runoff. With daily (and larger) time-steps, the night time and daytime rainfalls are combined and the total rainfall can evaporate if the potential evaporation for the day is sufficient. In

contrast, the hourly and 15-minute simulations can distinguish between daytime and night time conditions.

Table 8 shows the model performance in terms of the NSE and BIAS for each time-step. As expected, models using parameters optimised for a particular time-step out-performed

**Table 6** | Percentage of total rainfall in each component

% of total rainfall	Daily time-step		
	Daily Opt	Scaled Hourly Opt	Scaled 15-min Opt
$r_1$	12.20	2.60	8.50
$r_2$	0.00	0.00	0.00
$r_3$	17.90	23.90	16.90
$r_g$	32.10	34.00	31.90
Soil Evap	17.90	18.70	20.40
PET	19.90	20.80	22.40
% of total rainfall	Hourly time-step		
	Scaled Daily Opt	Hourly Opt	Scaled 15-min Opt
$r_1$	14.70	3.10	10.40
$r_2$	8.10	1.30	1.50
$r_3$	14.70	23.10	15.80
$r_g$	26.30	32.80	29.80
Soil Evap	28.80	31.80	34.10
PET	7.50	7.80	8.40
% of total rainfall	15-minute time-step		
	Scaled Daily Opt	Scaled Hourly Opt	15-min Opt
$r_1$	14.90	3.20	10.70
$r_2$	11.50	3.30	3.30
$r_3$	13.50	22.40	15.40
$r_g$	24.20	31.80	28.90
Soil Evap	29.70	33.00	34.90
PET	6.00	6.30	6.80

the models using parameters that were optimised for a different time-step and scaled as appropriate. The model using the 15-minute scaled parameters performed well, nearly matching the performance of the model using the optimised hourly parameters for the hourly time-step and out-performed the model using the scaled hourly optimised parameters for the daily model runs. The model performance using the daily parameters dropped as parameters were scaled from daily to 15-minute time-steps (NSE was equal to 0.8 for daily runs and dropped to 0.33 for 15-minute runs). Figure 8 shows the stream-flow time series for the daily and 15-minute calibrated model. The model using hourly calibrated parameters was excluded as it is nearly identical to the 15-minute calibrated model. This figure also shows the model is able to match the observed hydrograph for all the time-steps considered.

## SUMMARY AND CONCLUSIONS

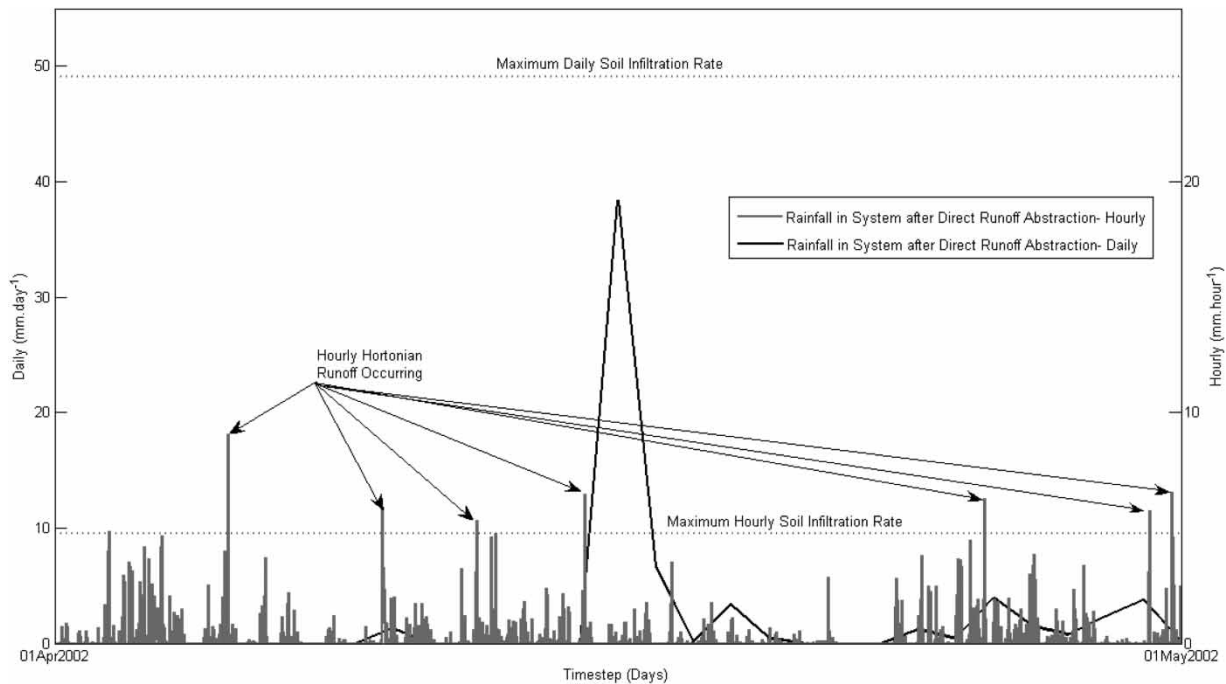
This study used the HDMR tool to calculate the sensitivity indices of the lumped conceptual SMARG rainfall-runoff model and investigate how the parameter uncertainty varied with respect to the modelling time-step and the hydrological regime. Three different flow regimes (high, low and a year of mixed flow period), two evaluation metrics (Nash Sutcliffe efficiency and mean bias) and three different model time-steps (daily, hourly and 15 minute) were used in this analysis.

The parameters that are most influential depend on the time-step and flow regime considered. The consistent insensitivity of the model to the mass balance control parameters (e.g. evaporation decay coefficient (C) and the maximum soil moisture infiltration rate (Y)), indicated by the HDMR



**Table 7** | Percentage of outflow accounted by each flow component (direct runoff, Hortonian runoff, subsurface runoff and groundwater flow)

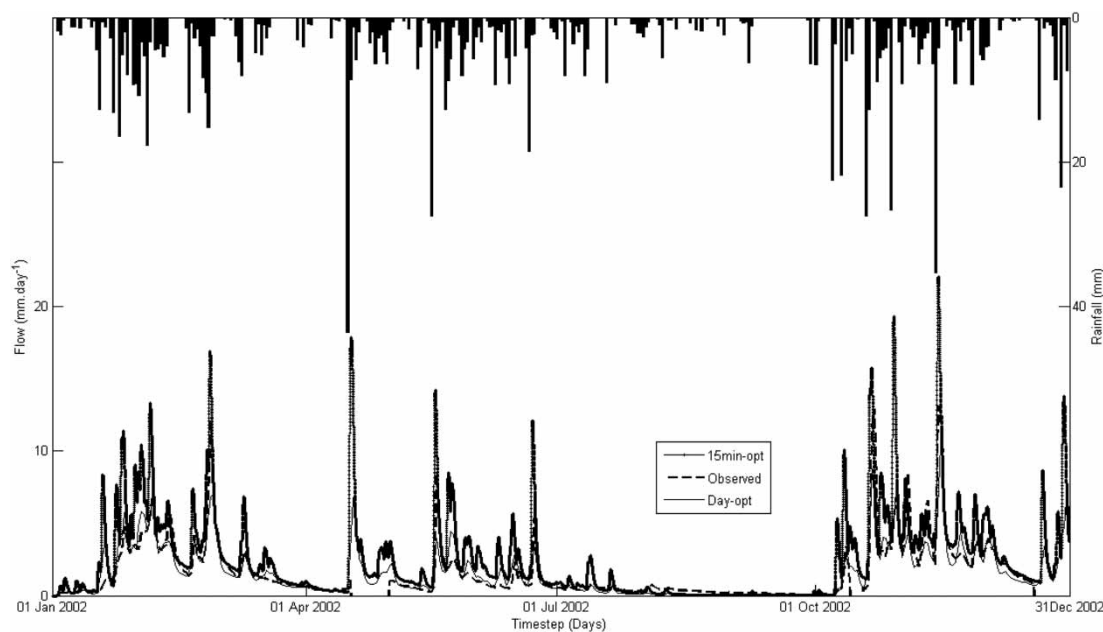
% of outflow	Daily time-step		
	Daily Opt	Scaled Hourly Opt	Scaled 15-min Opt
$r_1$	19.60	4.30	14.80
$r_2$	0.00	0.00	0.00
$r_3$	28.80	39.60	29.60
$r_g$	51.60	56.10	55.60
% of outflow	Hourly time-step		
	Scaled Daily Opt	Hourly Opt	Scaled 15-min Opt
$r_1$	23.10	5.20	18.10
$r_2$	12.70	2.20	2.60
$r_3$	23.00	38.30	27.50
$r_g$	41.20	54.30	51.80
% of outflow	15-minute time-step		
	Scaled Daily Opt	Scaled Hourly Opt	15-min Opt
$r_1$	23.30	5.30	18.40
$r_2$	18.00	5.40	5.70
$r_3$	21.10	36.90	26.30
$r_g$	37.70	52.40	49.60



**Figure 7** | Generation of surface runoff via Hortonian runoff pathway,  $r_2$ .

**Table 8** | Model performance with parameters scaled in a dimensional consistent way

	Daily time-step		
	Daily Opt	Scaled Hourly Opt	Scaled 15-min Opt
NSE	0.80	0.52	0.56
BIAS (mm/day)	0.06	0.07	0.15
	Hourly time-step		
	Scaled Daily Opt	Hourly Opt	Scaled 15-min Opt
NSE	0.38	0.84	0.83
BIAS (mm/hour)	0.65	0.22	0.24
	15-minute time-step		
	Scaled Daily Opt	Scaled Hourly Opt	15-min Opt
NSE	0.33	0.70	0.83
BIAS (mm/15 min)	0.16	0.13	0.06

**Figure 8** | Modelled flow using daily and 15-minute-based optimum parameters (rainfall is shown at the top of the figure).

results, suggests that the SMARG model may be over parameterised for this catchment. For applications in which the temporal distribution of evaporation and rainfall are important, a smaller time-step interval should be used (provided good quality input data are available).

The study shows that the model output is sensitive to the routing component parameters during high flow periods,

while during low flow periods, the soil storage capacity parameter has the most influence. The model parameters are biased towards the range of flow regimes in the calibration period, i.e. model calibration using high flow periods should be used for flood forecasting objectives.

Parameters of a nonlinear conceptual model, optimised at one time-step, should not be extrapolated, even if they are

dimensionally scaled to different time-steps. Similar conclusions were drawn by Littlewood & Croke (2008). Using scaled SMARG model parameters values from one time-step resulted in significantly different amounts of water being routed through each component of the model, even though the total combined outflow was similar in each case. This can be problematic if the model is used for flow pathway separation.

Future work should investigate whether or not the parameters found to be insensitive are common across a wide range of catchments and hydro-climatic gradients. Following the proposed simulation schemes by Clarke & Kavetski (2010), the use of time-step independent parameters in the SMARG model should be investigated.

## ACKNOWLEDGEMENTS

The authors are thankful for financial support from the following sources, UCD Ad Astra Scholarship, Urban Institute UCD and the Science Foundation Ireland (grant 07/RFP/ENMF292). The authors would like to express their thanks to Met Eireann, especially to Ciaran Commins for providing the meteorological data, and to the OPW Hydrometric Section, in particular to Kenneth Freehill for supplying the hydrometric data. The authors are grateful to Dr Tilo Ziehn for providing the GUI-HDMR software and assistance when required. Finally the authors would like to express their gratitude to Dr Ilias Pechlivanidis, and another anonymous reviewer for their constructive comments which improved the clarity of the manuscript.

## REFERENCES

- Bastidas, L. A., Gupta, H. V., Sorooshian, S., Shuttleworth, W. J. & Yang, Z. L. 1999 Sensitivity analysis of a land surface scheme using multicriteria methods. *Journal of Geophysical Research* **104** (D16), 19481–19490.
- Bates, B. C., Kundzewics, Z. W., Wu, S. & Palutikof, J. P. 2008 *Climate Change and Water*. Technical Paper of the Intergovernmental Panel on Climate Change, IPCC Secretariat, Genève.
- Bell, V. A. & Moore, R. J. 1998 A grid-based distributed flood forecasting model for use with weather radar data: Part 2. Case studies. *Hydrology and Earth System Sciences* **2**, 283–298.
- Blanchard, S., Papadopoulo, T., Benar, C. -G., Voges, N., Clerc, M., Benali, H., Warnking, J., David, O. & Wendling, F. 2011 Relationship between flow and metabolism in BOLD signals: insights from biophysical models. *Brain Topography* **24**, 40–53.
- Cibin, R., Sudheer, K. P. & Chaubey, I. 2010 Sensitivity and identifiability of stream flow generation parameters of the SWAT model. *Hydrological Processes* **24**, 1133–1148.
- Clarke, M. P. & Kavetski, D. 2010 Ancient numerical daemons of conceptual hydrological modelling: 1. Fidelity and efficiency of time stepping schemes. *Water Resources Research* **46**, W10510.
- Davis, M. J., Skodje, R. T. & Tomlin, A. S. 2011 Global sensitivity of chemical- kinetic reaction mechanisms: construction and deconstruction of the probability density function. *Journal of Physical Chemistry A* **115**, 1556–1578.
- Demaria, E. M., Nijssen, B. & Wagener, T. 2007 Monte Carlo sensitivity analysis of land surface parameters using the variable infiltration capacity model. *Journal of Geophysical Research* **112**, D11113.
- Dunne, S., Hanafin, J., Lynch, P., McGrath, R., Nishimura, E., Nolan, P., Venkata Ratnam, J., Semmler, T., Sweeney, C., Varghese, S. & Wang, S. 2008 Ireland in a Warmer World: Scientific Predictions of the Irish Climate in the Twenty-First Century. Report. Met Eireann, Dublin, Ireland.
- Fenicia, F., Savenije, H. H. G., Matgen, P. & Pfister, L. 2008 Understanding catchment behavior through stepwise model concept improvement. *Water Resources Research* **44**, W01402.
- Hossain, F., Anagnostou, E. N., Dinku, T. & Borga, M. 2004 Hydrological model sensitivity to parameter and radar rainfall estimation uncertainty. *Hydrological Processes* **18**, 3277–3291.
- Kavetski, D. & Clarke, M. P. 2010 Ancient numerical daemons of conceptual hydrological modelling: 2. Impact of time stepping schemes on model analysis and prediction. *Water Resources Research* **46**, W10511.
- Khan, H. 1986 Conceptual Modelling of rainfall-runoff systems. M. Eng. Thesis. National University of Ireland, Galway.
- Li, G., Wang, W., Rabitz, H., Wang, S. & Jaffé, P. 2002 Global uncertainty assessments by high dimensional model representations (HDMR). *Chemical Engineering Science* **57**, 4445–4460.
- Liang, G. C. 1992 A Note on the Revised SMAR Model. Workshop memorandum. Department of Engineering Hydrology, National University College of Ireland, Galway (Unpublished).
- Littlewood, I. G. & Croke, F. W. 2008 Data time-step dependency of conceptual rainfall- streamflow model parameters. *Hydrological Sciences Journal* **53**, 685–695.
- Littlewood, I. G. 2007 Rainfall–streamflow models for ungauged basins: uncertainty due to modelling time-step. In: *Proceedings Eleventh Biennial Conference of the EuroMediterranean Network of Experimental Basins (ERB), Luxembourg, 20–23 September 2006* (L. Pfister & L. Hoffmann, eds). UNESCO Technical Documents in Hydrology, Series no. 81. UNESCO, Geneva, pp. 149–155.

- McIntyre, N. & Al-Qurashi, A. 2009 Performance of ten rainfall-runoff models applied to an arid catchment in Oman. *Environmental Modelling & Software* **24**, 726–738.
- Min, S. -K., Zhang, X., Zwiers, F. W. & Hegeri, G. C. 2011 Human contribution to more-intense precipitation extremes. *Nature* **470**, 378–381.
- Moreda, F., Koren, V., Zhang, Z., Reed, S. & Smith, M. 2006 Parameterization of distributed hydrological models: learning from the experiences of lumped modelling. *Journal of Hydrology* **320**, 218–237.
- Nash, J. E. & Sutcliffe, J. V. 1970 River flow forecasting through conceptual models, Part I – A discussion of principles. *Journal of Hydrology* **10**, 282–290.
- O'Connell, P. E., Nash, J. E. & Farrell, J. P. 1970 River Flow forecasting through conceptual models. Part 2: The Brosna catchment at Febrane. *Journal of Hydrology* **10**, 317–329.
- Pall, P., Aina, T., Stone, D. A., Stott, P. A., Nozawa, T., Hilberts, A. G. J., Lobmann, D. & Allen, M. R. 2011 Anthropogenic greenhouse gas contribution to flood risk in England and Wales in autumn 2000. *Nature* **470**, 382–385.
- Pechlivanidis, I. G., McIntyre, N. R. & Wheeler, H. S. 2010 Calibration of the semi-distributed PDM rainfall-runoff model in the Upper Lee catchment, UK. *Journal of Hydrology* **386**, 198–209.
- Rabitz, H., Alis, Ö. F., Shorter, J. & Shim, K. 1999 Efficient input-output model representations. *Computer Physics Communications* **117**, 11–20.
- Refsgaard, J. C. & Knudsen, J. 1996 Operation validation and intercomparison of different types of hydrological models. *Water Resources Research* **32**, 2189–2202.
- Saltelli, A. 2000 Fortune and future of sensitivity analysis. In: *Sensitivity Analysis* (A. Saltelli, K. Chan & E. M. Scott, eds). Wiley, Chichester, pp. 421–426.
- Saltelli, A. 2002 Making best use of model evaluations to compute sensitivity indices. *Computer Physics Communications* **145**, 280–297.
- Schoups, G., Vrugt, J. A., Fenicia, F. & van de Giesen, N. C. 2010 Corruption of accuracy and efficiency of Markov chain Monte Carlo simulation by inaccurate numerical implementation of conceptual hydrologic models. *Water Resources Research* **46**, pW10530.
- Sieber, A. & Uhlenbrook, S. 2005 Sensitivity analysis of a distributed catchment model to verify the model structure. *Journal of Hydrology* **310**, 216–235.
- Skodje, R. T., Tomlin, A. S., Klippenstein, S. J., Harding, L. B. & Davis, M. J. 2010 Theoretical validation of chemical kinetic mechanisms: combustion of methanol. *Journal of Physical Chemistry A* **114**, 8286–8301.
- Sobol, I. M. 1993 Sensitivity analysis for non-linear mathematical models. *Mathematical Modeling & Computational Experiment* **1**, 407–414.
- Sobol, I. M. 2001 Global sensitivity indices for nonlinear mathematical models and their Monte Carlo estimates. *Mathematics and Computers in Simulation* **55**, 271–280.
- Spear, R. C. & Hornberger, G. M. 1981 A technical note on the SPS energy analysis of Herendeen et al. *Space Solar Power Review* **2**, 305–306.
- Tan, B. Q. & O'Connor, K. M. 1996 Application of an empirical infiltration equation in the SMAR conceptual model. *Journal of Hydrology* **185**, 275–295.
- Tang, Y., Reed, P., van Werkhoven, K. & Wagener, T. 2007a Advancing the identification and evaluation of distributed rainfall-runoff models using global sensitivity analysis. *Water Resources Research* **43**, W06415.
- Tang, Y., Reed, P., Wagener, T. & van Werkhoven, K. 2007b Comparing sensitivity analysis methods to advance lumped watershed model identification and evaluation. *Hydrology and Earth System Sciences* **11**, 793–817.
- Uhlenbrook, S., Seibert, J., Leibundgut, C. & Rodhe, A. 1999 Prediction uncertainty of conceptual rainfall-runoff models caused by problems in identifying model parameters and structure. *Hydrological Sciences* **44**, 779–797.
- USEPA 2010 *Better Assessment Science Integrating point and Nonpoint Sources (BASINS)*. User Manual, Version 3.0. EPA-823-C-01-001, Office of Water, Washington, DC.
- van Werkhoven, K., Wagener, T., Reed, P. & Tang, Y. 2008 Characterization of watershed model behaviour across a hydroclimatic gradient. *Water Resources Research* **44**, W01429.
- van Werkhoven, K., Wagener, T., Reed, P. & Tang, Y. 2009 Sensitivity-guided reduction of parametric dimensionality for multi-objective calibration of watershed models. *Advances in Water Resources* **32**, 1154–1169.
- Wagener, T., van Werkhoven, K., Reed, P. & Tang, Y. 2009 Multiobjective sensitivity analysis to understand the information content in streamflow observations for distributed watershed modelling. *Water Resources Research* **45**, W02501.
- Yatheendradas, S., Wagener, T., Gupta, H., Unkrich, C., Goodrich, D., Schaffner, M. & Stewart, A. 2008 Understanding uncertainty in distributed flash flood forecasting for semiarid regions. *Water Resources Research* **44**, W05S19.
- Younger, P. M., Freer, J. E. & Beven, K. J. 2009 Detecting the effects of spatial variability of rainfall on hydrological modelling within an uncertainty analysis framework. *Hydrological Processes* **23**, 1988–2003.
- Ziehn, T. & Tomlin, A. S. 2008a Global sensitivity analysis of a 3D street canyon model—part I: the development of high dimensional model representations. *Atmospheric Environment* **42**, 1857–1873.
- Ziehn, T. & Tomlin, A. S. 2008b A global sensitivity study of sulphur chemistry in a premixed methane flame model using HDMR. *International Journal of Chemical Kinetics* **40**, 742–753.
- Ziehn, T., Dixon, N. S. & Tomlin, A. S. 2009 The effects of parametric uncertainties in simulations of a reactive plume using a Lagrangian stochastic model. *Atmospheric Environment* **43**, 5978–5988.